IDETC/CIE 2008
ASME 2008 International Design Engineering Technical Conferences and Computers and Information in Engineering Conference
August 3-6, 2008, New York, NY, USA

DETC2008-49478

CONTOUR-CRAFTING-CARTESIAN-CABLE ROBOT SYSTEM CONCEPTS: WORKSPACE AND STIFFNESS COMPARISONS

Robert L. Williams II[1], Ming Xin[1], Paul Bosscher[2]
Department of Mechanical Engineering, Ohio University, Athens, Ohio 45701[1]
Government Communication Systems Division, Harris Corporation, Palm Bay, FL, 32905[2]

Email: williar4@ohio.edu, ming.xin.1@ohio.edu, pbossche@harris.com

ABSTRACT

Contour crafting (CC) is a new technology that is proposed for construction. Formerly we presented a cable-suspended robot to implement CC technology with Cartesian motion. The current paper proposes an improved Contour-Crafting-Cartesian-Cable (C^4) robot. Although the new concept is preferable in structural design, here we compare the original and improved C^4 robot concepts with regard to kinematics, workspace, and stiffness.

KEYWORDS

Contour crafting, cable-suspended robot, C^4 robot, translation-only, workspace, stiffness.

1. INTRODUCTION

Khoshnevis ([1], [2]) proposes contour crafting for construction of single-family dwellings and other buildings. In [3] we proposed the Contour Crafting Cartesian Cable (C^4) robot to perform the Cartesian motions required in CC construction. Figure 1 shows the original C^4 robot (Concept A) and Figure 2 shows the improved C^4 robot (Concept B). Concept B has some structural design improvements, discussed in the next section. This paper formally compares the two concepts with regard to positive-cable-tension workspace and translational and rotational stiffness; we conclude with a recommendation considering tradeoffs in design.

2. C^4 ROBOT CONCEPTS

To obtain translation-only manipulation of a CC end-effector through large workspaces for construction, we proposed [3] the original C^4 robot, Figure 1. It consists of a rigid frame and an end-effector suspended from twelve active cables, grouped into four upper cables and eight lower cables. The eight lower cables occur in four pairs of parallel cables.

The pulleys for the lower cables are mounted on horizontal crossbars, oriented at 45º with respect to the adjacent horizontal frame members, where the width of each crossbar is equal to the width of the corresponding side of the end-effector (also oriented at 45º for all motions).

The upper cables support the end-effector weight, while the lower cables provide the required translation-only motion. For each pair of cables, the two cables are controlled to have the same length. A parallelogram is formed by each pair of cables and the corresponding crossbar and end-effector edge. By maintaining this parallelism, translation-only motion can be guaranteed [3]. This simplifies manipulator control and reduces the complexity of the forward kinematics solution.

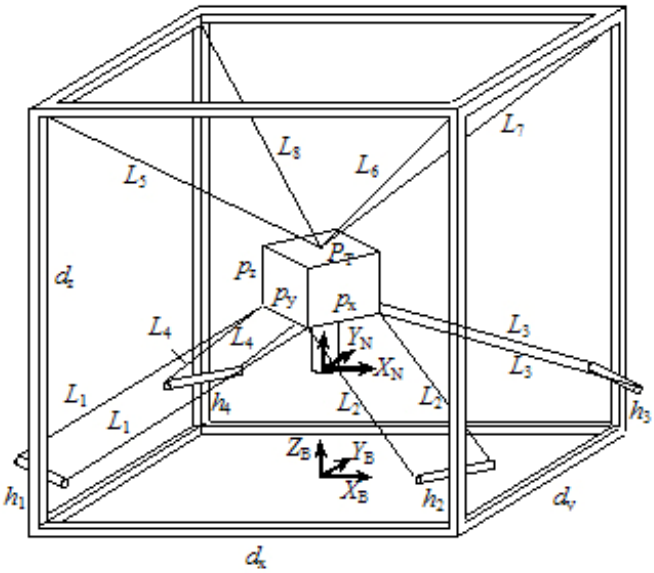

Figure 1. Original C^4 Robot, Concept A

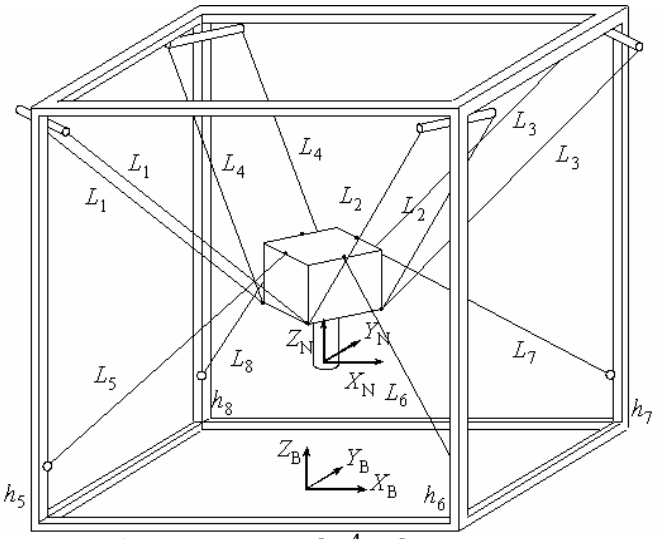

Figure 2. Improved C[4] Robot, Concept B

To prevent cable interference with the building being constructed, the 45º horizontal crossbars are actuated vertically (heights h_i, i=1,2,3,4 are independently-controlled variables). This presents a challenging design problem. To improve the C[4] robot, therefore, we propose Concept B in Figure 2. In Concept B, the 45º horizontal crossbars are fixed to the top of the frame and thus do not need to be actuated vertically. Instead, the single-cable pulleys are actuated vertically as the construction grows (heights h_j, j=5,6,7,8 are independently-controlled variables). This is far easier to design, construct, and operate than Concept A's variable double pulleys. Concept B still provides translation-only motion, but the parallel cables are now mounted from the frame top. Also, the cables have been crossed (the lower cables connect to the end-effector top and the upper cables connect to the end-effector bottom), which leads to superior rotational stiffness compared to Concept A (studied in this paper).

Figures 3 and 4 present the C[4] robot Concepts A and B in simulated CC construction tasks.

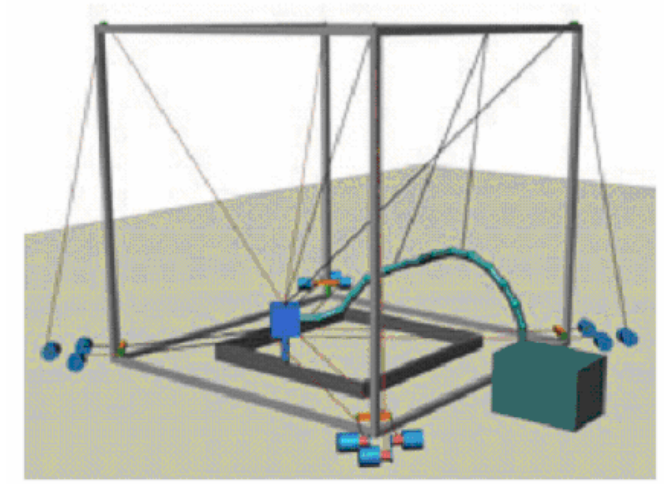

Figure 3. Concept A C[4] Robot in Construction

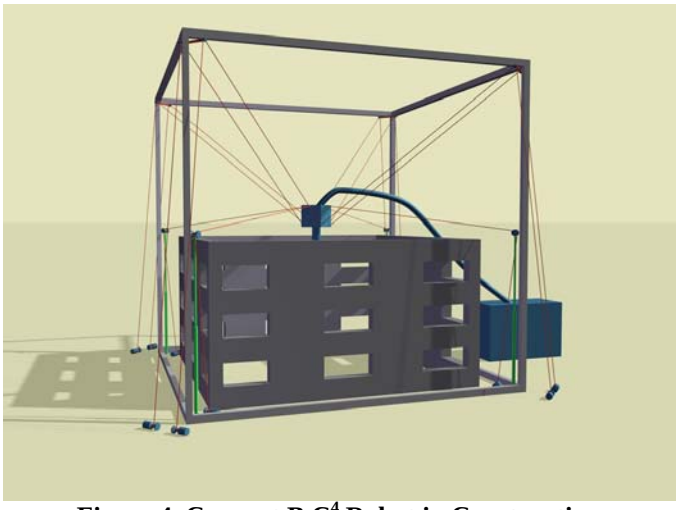

Figure 4. Concept B C[4] Robot in Construction

3. C[4] ROBOT KINEMATICS

The inverse and forward position kinematics equations and solutions are presented in [3] for the C[4] robot, Concept A. As expected for most parallel robots, the inverse position solution is straightforward and not computationally demanding. However, unlike most parallel robots, the forward position kinematics solution is also straightforward since we can use the virtual cable method [3] which only requires the intersection of three spheres (a closed-form solution, [4]) for solution.

The kinematics solutions are very similar for C[4] robot Concepts A and B and thus cannot serve to distinguish between the two concepts. Therefore, we now move on to workspace and stiffness comparisons.

4. C[4] ROBOT WORKSPACE

Workspace is an important criterion to evaluate the C[4] robot concepts. We define the C[4] robot workspace as the set of all *x-y-z* positions that the CC nozzle tip point can attain while maintaining full constraint of the end-effector and being able to exert a specified set of forces and moments on its surroundings with all non-negative cable tensions and without any of the cables exceeding their upper tension limits. This has also been termed the "wrench-feasible workspace" of a cable robot [5].

In order to investigate the workspace of this robot, an example geometry was chosen and the workspace generated numerically using MATLAB. This example geometry consists of a 1 m cube end-effector manipulated within a 50 m cube frame. To match the end-effector dimensions, each of the horizontal crossbars is 1 m wide. The end-effector has a mass of 1000 *N* and the maximum allowable tension in a cable is 10 *kN*. The space within the robot's frame is discretized into 2 m cubes. In addition to supporting the weight of the end-effector, at each position the robot is required to exert a force of ±450 N in the *x*, *y* and *z* directions and a moment of ±200 N·m about the *x*, *y* and *z* axes. For each of these loading conditions the tensions in the cables are determined. The statics equations of the manipulator are underdetermined, thus the cable tensions cannot be determined uniquely. To resolve this we use

MATLAB function *lsqnonneg*, which solves the least-squares problem for static equilibrium subject to non-negative cable tensions. The maximum single cable tension is determined for each individual loading condition, and then the overall maximum tension (the maximum single cable tension over all of the loading conditions) is determined for each position.

This wrench-feasible workspace has already been presented for the C^4 robot Concept A in [3]. For comparison, this section presents for the first time the workspace of Concept B, subject to the same simulation parameters. The Concept A workspaces are repeated here from [3], side-by-side with the new Concept B workspaces for easy comparison and discussion.

After the overall workspaces are presented, we consider detailed workspaces with different end-effector heights z (z = 3, 28, 43) and different variable pulley heights h (h = 0, 25, 40). All height units in this section are m. Since the end-effector is expected to operate most in the vicinity of the pulley heights h, we present workspace slices focusing on that. For completeness, we also present partial workspaces from the variable pulley heights on up to the maximum height in the frame.

Figure 5 shows the overall workspaces for Concept A and Concept B (below, the Concept A workspaces are always on the left and the corresponding Concept B workspaces on the right). Here, the horizontal crossbar of Concept A and pulleys of Concept B are both at the frame bottom (h = 0). In the diagrams, each box has been assigned with a color representing the maximum cable tensions acting in this position. In both Figures 5, we find that both concepts' workspaces fill the frame, and their workspace is symmetrical (because the C^4 robot is symmetrical). However, the workspace of Concept B is superior to Concept A because the Concept B workspace fills the cube more completely. The Concept A workspace is reduced in the middle of the frame. Also, the Concept B workspace is largely blue or cyan boxes and more of the Concept A workspace is yellow, orange or red boxes. So the cable tensions acted on this workspace of Concept A are greater than the ones of Concept B, making Concept B again preferable.

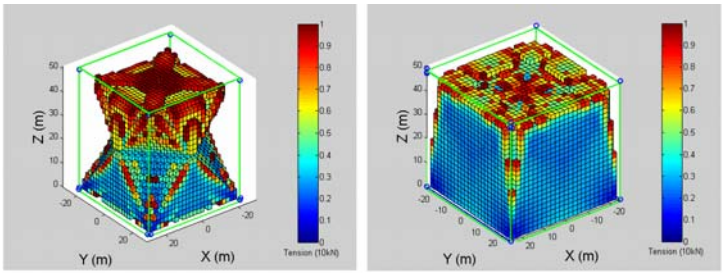

Figure 5. Overall Wrench-Feasible Workspaces (Concept A left, Concept B right)

Figure 6 shows quarter sections of the overall workspaces. Both concepts' internal workspace is filled with blue or cyan boxes. Therefore, the cable tensions in the interior of the workspace are relatively low, desirable results for both concepts.

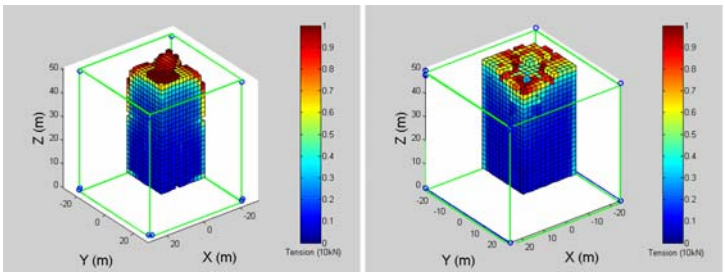

Figure 6. Quarter Section Workspaces

Figure 7 shows both concepts' workspaces with variable pulleys at minimum height h = 0 and working in this vertical vicinity. The Concept B workspace slice is better than Concept A, although both internal workspaces generally have low cable tensions. The four edges of the Concept A slice (left) have high cable tensions and some space is eliminated from the workspace. Compared to Concept A, the Concept B workspace keeps its workspace slice intact; also, most of the slice is blue with some cyan appearing at the four edges.

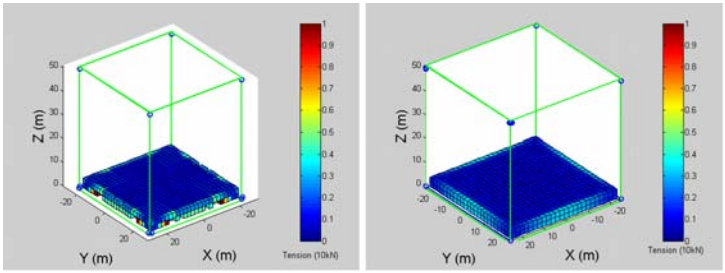

Figure 7. Low Workspace Slices with h = 0 m

Figure 8 shows the workspaces with the variable-height pulleys raised to h = 25 m. The workspace of Concept A has some improvements: the workspace is enlarged compared to the upper part of Concept A in Figure 5, and the surrounding cable tensions are not as high as the upper part of Concept A in Figure 5. However, Concept A still lost some workspace and its surrounding cable tensions are still higher than Concept B, although Concept B lost some space towards the top. Therefore, Concept B maintains its superior aspect in this layer of the workspace comparison.

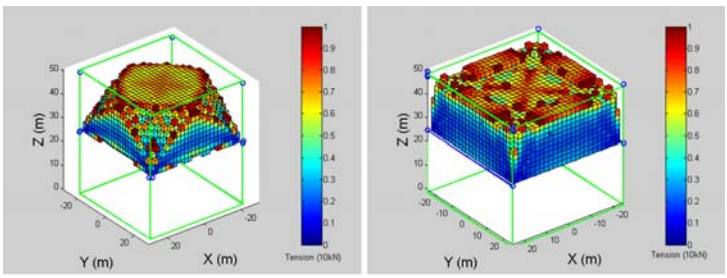

Figure 8. Mid-Workspaces with h = 25 m

Figure 9 shows both concept workspace slices at h = 25 m. These two diagrams are very similar to the slices in Figure 7. The internal workspace cable tensions are low for both

concepts. The four edges of the Concept A workspace have high cable tensions, and some workspace was eliminated because of high cable tensions. Concept B keeps low cable tensions in most of this workspace slice, and higher cable tensions (> 4kN) only occur in part of the four edges. Therefore, the Concept B workspace is again better than Concept A here.

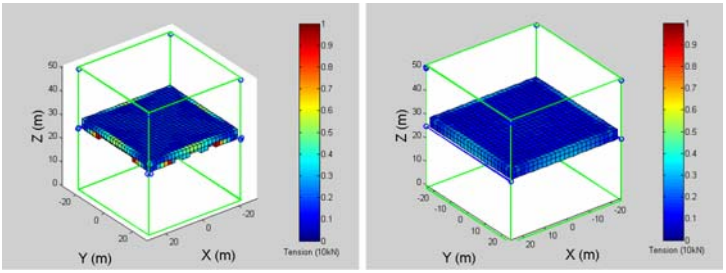

Figure 9. Mid-Workspace Slices with *h* = 25 m

Figure 10 shows both concept workspaces in a third layer with h = 40 m. The internal cable tensions in the top slice of Concept A are increasing from the surrounding space to the center; the center spot is eliminated because of high cable tensions. Compared to Concept A, the cable tensions of Concept B internal workspace are lower. However, in this section of workspace, the Concept A workspace is thicker than Concept B because Concept A has four 2m-slices of workspace, whereas Concept B only has three slices (the fourth slices exist only in fragmented positions with high cable tensions), but these are broader than Concept A. Therefore, both concepts have their own advantages and are about even at this level.

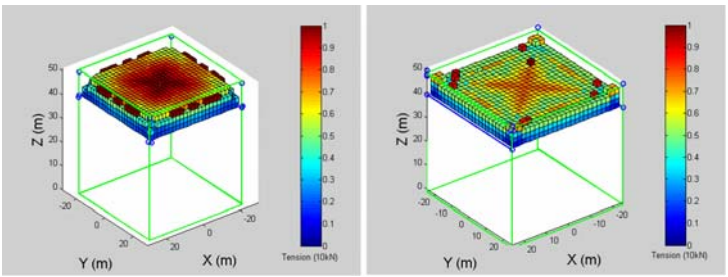

Figure 10. High Workspaces with *h* = 40 m

Figure 11 shows both concept workspace slices at h = 40 m. Both diagrams show desirable aspects: low cable tensions and intact workspace slices. Concept B's workspace is slightly bigger.

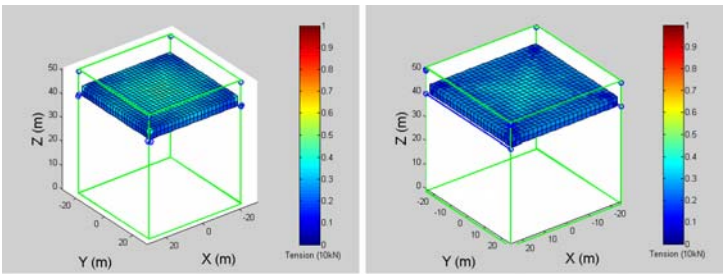

Figure 11. High Workspace Slices with *h* = 40 m

5. C^4 ROBOT STIFFNESS

Translational and rotational stiffness is the ability of an object to resist translational and rotational deflections when forces and moments are exerted on it. High C^4 robot stiffness is generally preferable to resist unwanted deflections resulting from disturbances in the construction environment and to maintain translational-only motion at all times. A stiffness study was first presented for cable robots (the NIST RoboCrane) in [6]. Translational stiffness units are N/m and rotational stiffness units are Nm/rad.

The stiffness equation in Cartesian space for the overall robot is [7]:

$$K = J\left[k_i\right]_{diag} J^T \tag{1}$$

K is the Cartesian stiffness matrix and J is the Jacobian matrix of the C^4 robot [3]. $[k_i]_{diag}$ is a 12x12 diagonal matrix, with diagonal terms k_i from (2).

$$k_i = \frac{EA}{L_i} \quad (i = 1, 2, 3, \cdots, 12) \tag{2}$$

E is Young's modulus of the cable material, A is the cable cross-sectional area, and L_i are the variable lengths of the cables. In the simulations of this section we assume steel cables ($E = 200\times10^9\, N/m^2$) of 2 cm diameter.

The Jacobian matrix is 6x12 and its transpose matrix is 12x6. $[k_i]_{diag}$ is a 12x12 diagonal matrix. Thus, matrix K is a 6x6 square matrix that can be divided into four 3x3 submatrices:

$$K = \begin{bmatrix} [I]_{3x3} & [II]_{3x3} \\ [III]_{3x3} & [IV]_{3x3} \end{bmatrix}_{6x6} \tag{3}$$

In (3), the structure of K is as follows: the submatrix $[I]_{3x3}$ is the C^4 robot translational stiffness matrix and the submatrix $[IV]_{3x3}$ is the C^4 robot rotational stiffness matrix. The submatrices $[II]_{3x3}$ and $[III]_{3x3}$ are a pair of transpose matrices relating the coupling between translational and rotational stiffnesses.

Translational and rotational stiffness depends on the end-effector position, so sample positions are chosen to evaluate the C^4 robot stiffness. Three different variable pulley heights are chosen: h = 0, h = 15 and h = 30. The heights of the end-effector nozzle are z = 3, z = 18 and z = 33 (all height units are m in this section), i.e. always 3 m higher than h in each case. In the three horizontal xy planes at the three z heights, nine sample points are selected as shown in Figure 12.

The translational and rotational matrices can easily be extracted from K but it is hard to evaluate and compare them. A good comparison alternative is to consider the Euclidian norms of two vectors separately, where the two vectors contain the eigenvalues of the translational and rotational submatrices. Referring to Figure 12, for both C^4 robot Concepts A and B, at any end-effector height z, the translational and rotational stiffness norms in the four yellow corner positions are identical (henceforth called "square"). The norms in four red midpoint

positions are identical (called “diamond”). The norm in the center is different from the above two types (called “cross”).

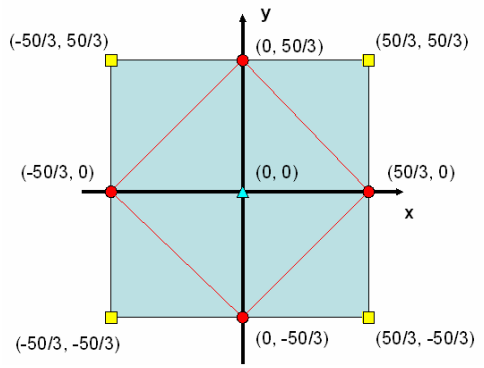

Figure 12. Horizontal Plane Sampling Points

5.1 Translational Stiffness Comparison

The translational stiffness simulation results will be presented in the vertical direction and horizontal planes, using the same parameters to compare C^4 robot Concepts A and B. For the vertical direction, the *x*, *y* coordinates are set into three classes as in Figure 12 and the end-effector *z* coordinate and variable pulley height *h* are changed. For the horizontal planes, the end-effector and pulley heights *z* and *h* are set, and the *x*, *y* coordinates are varied on each plane.

5.1.1 Vertical Direction Translational Stiffness

Figure 13 shows the translational stiffness results (the norm of the eigenvalues of the 3x3 translational matrix, as discussed above) in the vertical direction. In Figure 13, the solid line refers to Concept B and the dashed line to Concept A. Blue, red and green are assigned for three different norm locations: square, diamond, and cross. Three end-effector levels are shown on the same figure, starting from minimums of $z = 3$, $z = 18$, and $z = 33$ (with pulley heights $h = 0$, $h = 15$, and $h = 30$), extending to the workspace top in each case.

The translational stiffness of Concept A is greater than Concept B at lower heights; but with increasing height, the translational stiffness of Concept B becomes larger at some point. In all cases, the curves of Concepts A and B cross so the stiffness is superior for Concept A in some ranges and Concept B in others. It appears that Concept B translational stiffnesses are preferable to Concept A overall in the vertical direction, but this is not a strong conclusion. For instance, the C^4 robot will generally operate with the end-effector height near the variable pulley heights (as shown in Figures 3 and 4), making the Concept A stiffness generally preferable in Figure 13. For both Concepts A and B, the C^4 robot translational stiffness increases as the pulley heights increase.

5.1.2 Horizontal Plane Translational Stiffness

In this subsection we present comparisons of Concepts A and B translational stiffness matrix eigenvalue norms for six discrete planes: variable pulley height $h = 0$ with $z = 3$, 18, and 33; pulley height $h = 15$ with $z = 18$ and 33; and pulley height $h = 30$ with $z = 33$. As in the Workspace Section, here the translational stiffness results are presented side-by-side for easy comparison (Concept A always on the left and Concept B on the right). All diagrams have the same general shape: the stiffness in the edges is larger than the center. On the edges, the stiffness in the four corners is larger than the middles. In the figures, the color is gradually changing from red (high stiffness) to blue (lower stiffness). All results agree with Figure 13.

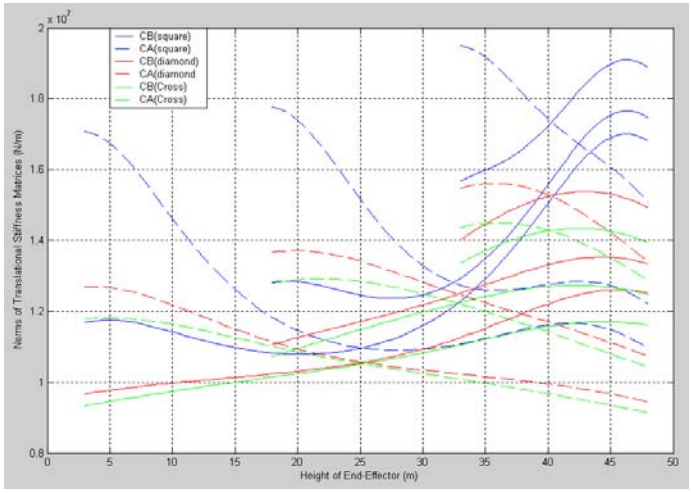

Figure 13. Translational Stiffness Vertical Dependence (Concept A dashed, Concept B solid)

Figure 14 shows the norms of translational stiffness matrices eigenvalues of Concepts A and B at $h = 0$ and $z = 3$. The highest stiffness occurs at the four corners of the plane. The Concept A stiffnesses (1 to 1.5 x10^7 N/m) are greater than Concept B (0.8 to 1 x10^7 N/m) in most cases. The four corner stiffnesses of Concept A are almost twice of that of Concept B. Therefore, Concept A is better than Concept B in this case.

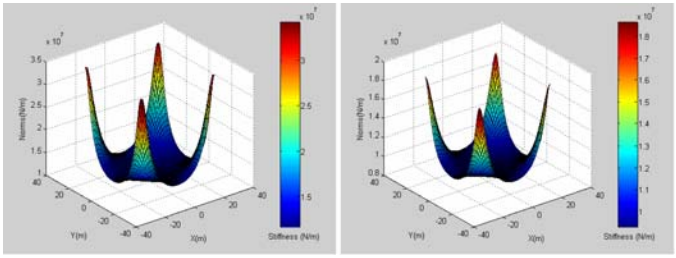

Figure 14. Translational Stiffness with $h = 0$ m, $z = 3$ m (Concept A left, Concept B right)

In Figure 15, the end-effector is raised ($z = 18$) and the pulley height is unchanged ($h = 0$). The lower limits for both concepts’ stiffnesses are increased. However, both upper limits decreased dramatically: 3.5 to 1.2 x10^7 N/m for Concept A and 2 to 1.1 x10^7 N/m for Concept B. Although the norm differences between both concepts are smaller than Figure 14, Concept A (1.05 to 1.08 x10^7 N/m) is still better than Concept B (0.98 to 1.02 x10^7 N/m). 1.08x10^7 N/m is blue in the colorbar of Concept A but it is dark orange in that of Concept B.

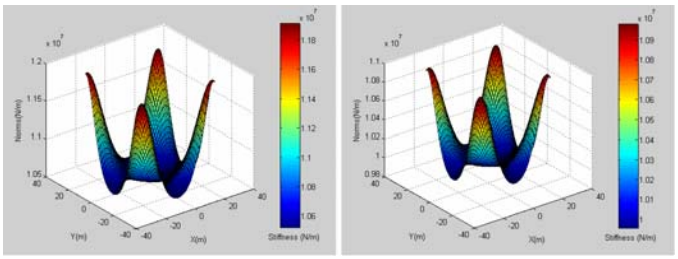

Figure 15. Translational Stiffness with *h* = 0 m, *z* = 18 m

In Figure 16 (*h* = 0 and *z* = 33), the translational stiffness norms of Concept B are greater than that of Concept A. Most Concept B norms are in the range 1 to 1.4x10^7 N/m, while those of Concept A are 0.9 to 1.2x10^7 N/m. The maximum stiffness of Concept A in the four corners (1.2x10^7 N/m) is less than the Concept B maximum (1.4x10^7 N/m). In this case Concept B is better than Concept A.

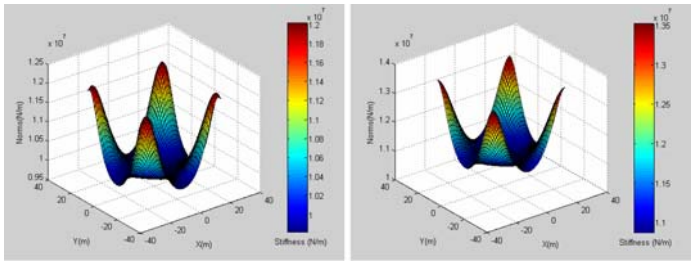

Figure 16. Translational Stiffness with *h* = 0 m, *z* = 33 m

Figures 17 are similar to Figures 14 because the relative height (3) of the end-effector in Figures 17 (*h* = 15, *z* = 18) is the same in Figure 14 (*h* = 0, *z* = 3). However, the lower translational stiffness norm limits of both concepts are increased. Concept B is more obvious, from 0.8 to 1x10^7 N/m. Since Figure 17 is similar to Figure 14, Concept A (left) is better than Concept B (right) in this case also.

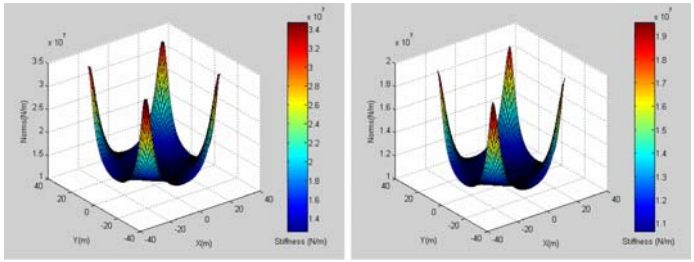

Figure 17. Translational Stiffness with *h* = 15 m, *z* = 18 m

In Figure 18 (*h* = 18 and *z* = 33) the norm upper limits of both concepts are decreased and their lower limits are increased compared with Figure 17. The Concept A range is 1.15 to 1.20x10^7 N/m, while that of Concept B is from 1.20 to 1.25x10^7 N/m. The maximum Concept A norm in the four corners (1.40x10^7 N/m) is less than that of Concept B (1.45x10^7 N/m). Thus, the Concept B is slightly better than Concept A here.

This verifies the curves in Figure 13, where the three Concept B curves (solid) go up after *z* = 32m, while the three Concept A curves (dashed) go down. At *z* = 33, the translational stiffness of Concept B is greater than that of Concept A.

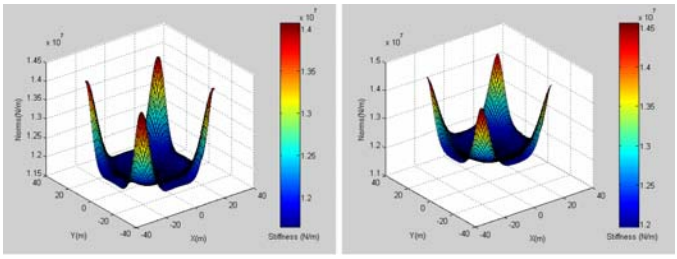

Figure 18. Translational Stiffness with *h* = 15 m, *z* = 33 m

In Figure 19, the limits of both concepts are increased. This situation is similar to Figures 14 and 17. Concept A (1.4 to 1.8x10^7 N/m) is slightly better than Concept B (1.3 to 1.5x10^7 N/m) at *h* = 30m and *z* = 33m. The maximum norm in the four corners of Concept A (3.4x10^7 N/m) is greater than that of Concept B (2.1x10^7 N/m).

In Figure 13, all three dashed curves that start from *z* = 33 are greater than three solid curves before *z* = 37, so lower than *z* = 37, the translational stiffness of Concept A is greater than Concept B, which agrees with Figure 19. Generally, the higher in the workspace, the greater the translational stiffness of Concept B compared to Concept A.

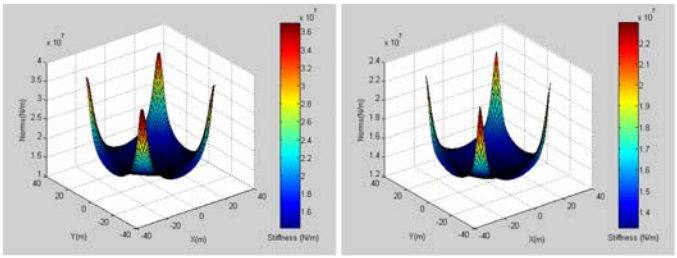

Figure 19. Translational Stiffness with *h* = 30 m, *z* = 33 m

5.2 Rotational Stiffness Comparison

The same parameters, ranges, and plot types from translational stiffness are now used to compare the rotational stiffness of C^4 robot Concepts A and B.

5.2.1 Vertical Direction Rotational Stiffness

Figure 20 shows the norms of the rotational stiffness matrix eigenvalues of both Concepts A and B in the vertical direction. The line styles and colors are the same as Figure 13. The Concept B rotational stiffness is almost always significantly greater than the rotational stiffness of Concept A. Moreover, the rotational stiffness of Concept B increases while that of Concept A decreases significantly as the end-effector and variable pulley heights increase. As the variable pulley height increases, the rotational stiffness of Concept B is increasingly larger than that of Concept A.

For the Concept B curves, there is generally a peak rotational stiffness value for some end-effector height. The Concept A curves are generally decreasing with end-effector

height. With regard to rotational stiffness, Concept B is much better than Concept A.

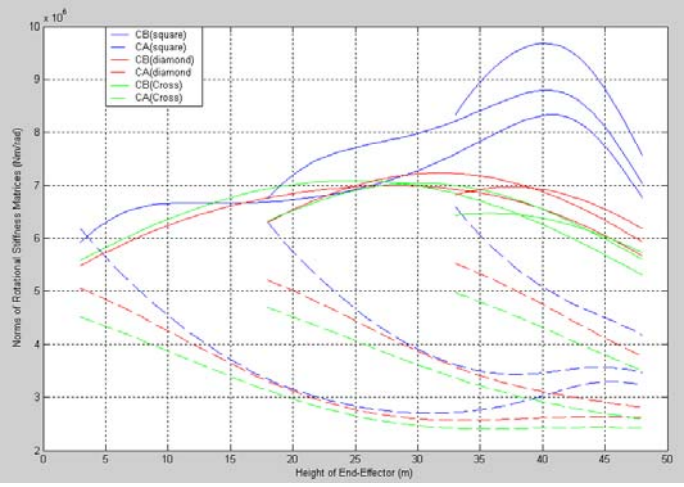

Figure 20. Rotational Stiffness Vertical Dependence (Concept A dashed, Concept B solid)

5.2.2 Horizontal Plane Rotational Stiffness

Figure 21 shows the Concepts A and B rotational stiffness for h = 0 and z = 3. Most Concept A stiffnesses (4.0 to 6.0x10^6 Nm/rad) are less than those of Concept B (5.5 to 6.3x10^6 Nm/rad). However, rotational stiffness of Concept A increases more than that of Concept B at the four corners. Within the range -17 < X, Y <17, the rotational stiffness of Concept B is greater than that of Concept A. Outside this range, the rotational stiffness of Concept A is greater than that of Concept B. Therefore, Concept A and Concept B are about even here.

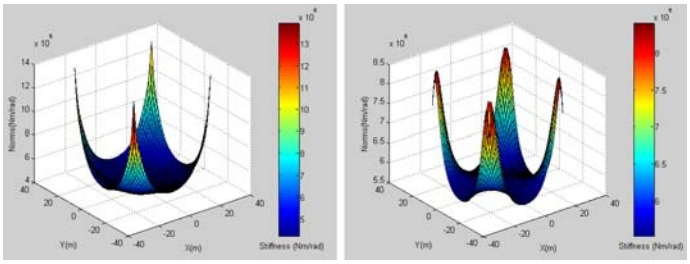

Figure 21. Rotational Stiffness with h = 0 m, z = 3 m

In Figure 22, the variable pulley height h = 0 is the same and the end-effector height is z = 18. Both concepts' stiffness upper limits decreased compared to Figure 21: Concept A, decreased from 13.0 to 3.8x10^6 Nm/rad and Concept B decreased less, from 8.0 to 6.8x10^6 Nm/rad. Concept B is preferable to Concept A here with regard to rotational stiffness.

Unlike all other rotational and translational stiffness figures above, the Concept B high stiffness norms are at the center and cover a large range, while the minimum norms occur at the four corners.

In Figure 23 (h = 0 and z = 18), the rotational stiffness of Concept B is greater than that of Concept A in all positions.

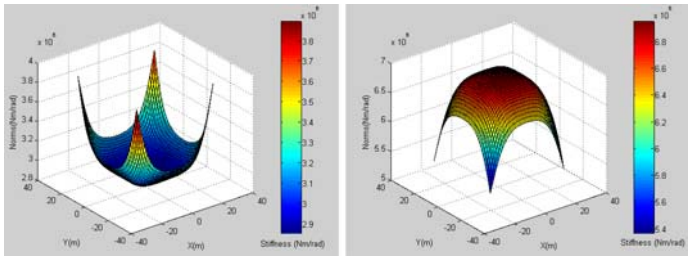

Figure 22. Rotational Stiffness with h = 0 m, z = 18 m

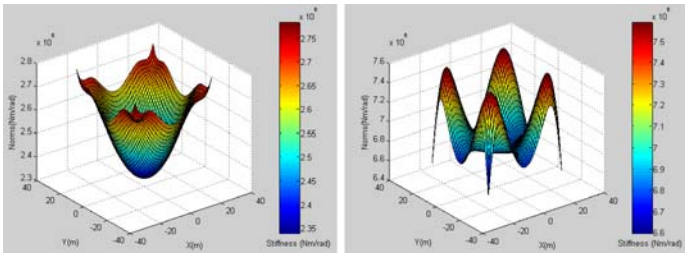

Figure 23. Rotational Stiffness with h = 0 m, z = 33 m

Figure 24 (h = 15 and z = 18) shows that the rotational stiffness norms Concept A (4.0 to 6.0x10^6 Nm/rad) are less than those of Concept B (6.0 to 6.8x10^6 Nm/rad), for most of the workspace range. But near the four corners the rotational stiffness of Concept A increases faster than that of Concept B. Similar to Figure 21, within the range -17 < X, Y <17, the rotational stiffness of Concept B is greater than that of Concept A. Outside this range, the rotational stiffness of Concept A is greater than that of Concept B. Therefore, Concept A and Concept B are about even here.

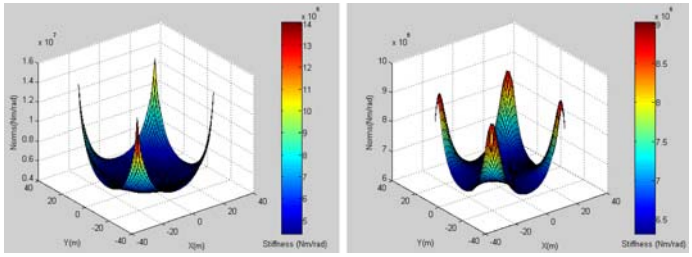

Figure 24. Rotational Stiffness with h = 15 m, z = 18 m

In Figure 25 (h = 15 and z = 33), the rotational stiffnesses of Concept B are significantly greater than those of Concept A in all positions.

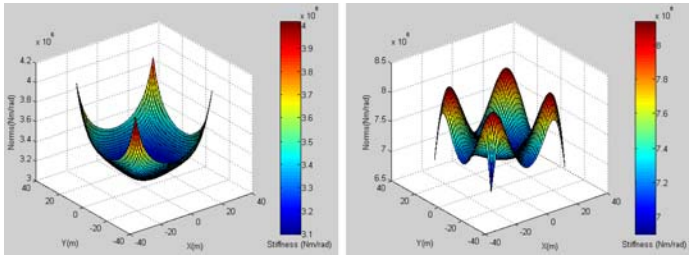

Figure 25. Rotational Stiffness with h = 15 m, z = 33 m

Figure 26 shows that the rotational stiffness norms of Concept A (4.0 to 6.0x10^6 Nm/rad) are less than Concept B (6.0 to 7.5x10^6 Nm/rad), for the most part. But near the four corners, the Concept A rotational stiffnesses are greater than those of Concept B. Similar to Figures 21 and 24, within the range -17 < X, Y <17, the rotational stiffness of Concept B is greater than that of Concept A. Outside this range, the rotational stiffness of Concept A is greater than that of Concept B. Therefore, Concept A and Concept B are about even here also.

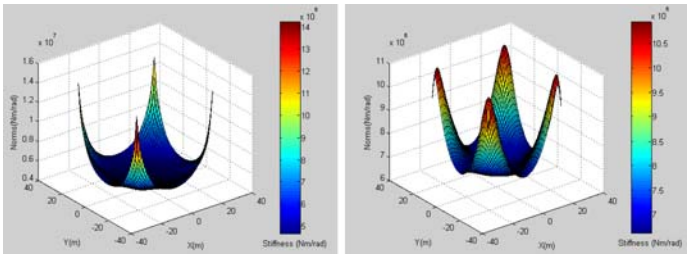

Figure 26. Rotational Stiffness with *h* = 30 m, *z* = 33 m

We find that several cases (Figures 21, 24 and 26; Figures 22 and 25) that have identical relative height of the pulleys and end-effector have similarities in their rotational stiffness plots.

6. C^4 ROBOT CONCEPTS A AND B COMPARISON

In Table I, we summarize the workspace and stiffness results comparison for Concepts A and B of the C^4 robot, to decide objectively which design is better. Workspace is an important characteristic of the C^4 robot. From Section 4, it is clear that the Concept B workspace is better than that of Concept A.

Stiffness is another important characteristic of the C^4 robot, the ability to resist unwanted disturbances. To evaluate Concepts A and B, both translational and rotational stiffnesses were considered. For each class, the stiffness was evaluated for both concepts based on planar and vertical directions. In planar translational stiffness, Concept A is better than Concept B; in vertical translational stiffness, both concepts are even. In planar rotational stiffness, Concept B is better than Concept A; in vertical rotational stiffness, Concept B is also better than Concept A.

7. CONCLUSION

In conclusion, after evaluating the workspace and stiffness of the C^4 robot, Concept B showed more advantages than Concept A. Therefore, Concept B is chosen for future development, including dynamics and controller work and scale prototype hardware development.

The fact that these workspace and stiffness objective results favor Concept B is great, because it has a major design improvement over Concept A: in Concept B, the double pulleys for the translational-only motion are fixed to the upper frame, while in Concept A these double pulleys must translate vertically, a big challenge in mechanical design. Also, the cables are crossed in Concept B but not Concept A, leading to superior rotational stiffness for Concept B.

Table I. Comparison Summary for C^4 Concepts A and B

			Concept A	Concept B
Workspace(m)	h = 0	50>=z>=0		✓
	h = 0	z = 3		✓
	h = 25	50>=z>=25		✓
	h = 25	z = 28		✓
	h = 40	50>=z>=40	✓	
	h = 40	z = 43	x	x
Translational Stiffness (planar)	h = 0	z = 3	✓	
	h = 0	z = 18	✓	
	h = 0	z = 33		✓
	h = 15	z = 18	✓	
	h = 15	z = 33		✓
	h = 30	z = 33	✓	
Rotational Stiffness (planar)	h = 0	z = 3	x	x
	h = 0	z = 18		✓
	h = 0	z = 33		✓
	h = 15	z = 18	x	x
	h = 15	z = 33		✓
	h = 30	z = 33	x	x
Translational Stiffness (Vertical)		Square	x	x
		Diamond	x	x
		Cross	x	x
Rotational Stiffness (Vertical)		Square		✓
		Diamond		✓
		Cross		✓

Notes: " ✓ " mean that this concept is better in this characteristic; "x"mean that both concepts are even in this characteristic

REFERENCES

[1] Khoshnevis, B., 2004. "Automated Construction by Contour Crafting – Related Robotics and Information Technologies". Journal of Automation in Construction – Special Issue: The best of ISARC 2002, 13(1): pp. 5 – 19.

[2] Khoshnevis, B., Russel, R., Kwon, H, and Bukkapatnam, S., "Crafting Large Prototypes," IEEE Robotics & Automation Magazine, pp. 33-42, September 2001.

[3] Bosscher, P., Williams II, R. L., Bryson, S and Castro-Lacouture, D., "Cable-suspended Robotic Contour Crafting System," in Proceedings of the 2006 ASME DETC/CIE conferences, (Philadelphia, Pennsylvania), DETC2006-99016, September 2006.

[4] Williams II, R. L., Albus, J. S., and Bostelman, R. V., 2004. "3D cable-based Cartesian metrology system". Journal of Robotic Systems, 21(5), pp. 237 – 257.

[5] Bosscher, P., 2004. "Disturbance robustness measures and wrench-feasible workspace generation techniques for cable-driven robots". PhD dissertation, Georgia Institute of Technology, Atlanta, GA, November.

[6] Unger, D., Dagalakis, N.G., Tsai, T.-M., and Lee, J.D., 1988, "Optimum stiffness study for a parallel link robot crane under horizontal force", 2nd Int. Symp. on Robotics and Manufacturing, Albuquerque NM: 1037-1046.

[7] Salisbury, J.K., 1980, "Active stiffness control of a manipulator in Cartesian coordinates," in *Proceedings of the 19th IEEE Conference on Decision and Control*, Albuquerque, NM, December: 87–97.